

Genetic susceptibility to schizophrenia through neuroinflammatory pathways is associated with retinal thickness: Findings from the UK-Biobank

Finn Rabe, PhD^{†1}, Lukasz Smigielski, PhD^{†2}, Foivos Georgiadis, MD¹, Nils Kallen, MD¹, Wolfgang Omlor, MD, PhD¹, Victoria Edkins, PhD¹, Matthias Kirschner, MD¹, Flurin Cathomas, MD¹, Edna Grünblatt, PhD^{2,3,4}, Steven Silverstein, PhD^{5,6,7,8}, Brittany Blose, MS^{5,6,7,8}, Daniel Barthelmes, MD, PhD⁹, Karen Schaal, MD¹⁰, Jose Rubio, MD, PhD^{11,12,13}, Todd Lencz, PhD^{11,12,13}, & Philipp Homan, MD, PhD^{1,3*}

¹ Department of Adult Psychiatry and Psychotherapy, University of Zurich, Zurich, Switzerland.

² Department of Child and Adolescent Psychiatry and Psychotherapy, University Hospital of Psychiatry Zurich, University of Zurich, Zurich, Switzerland.

³ Neuroscience Center Zurich, University of Zurich and ETH Zurich, Zurich, Switzerland.

⁴ Zurich Center for Integrative Human Physiology, University of Zurich, Zurich, Switzerland.

⁵ Department of Psychiatry, University of Rochester Medical Center, Rochester, New York, USA.

⁶ Department of Ophthalmology, University of Rochester Medical Center, Rochester, New York, USA.

⁷ Department of Neuroscience, University of Rochester Medical Center, Rochester, New York, USA.

⁸ Center for Visual Science, University of Rochester, Rochester, New York, USA.

⁹ Department of Ophthalmology, University Hospital Zurich, University of Zurich, Zurich, Switzerland.

¹⁰ Department of Ophthalmology, Inselspital University Hospital Bern, Bern, Switzerland.

¹¹ Institute of Behavioral Science, Feinstein Institutes for Medical Research, Manhasset, NY, USA.

¹² Division of Psychiatry Research, Zucker Hillside Hospital, Northwell Health, New York, NY, USA.

¹³ Department of Psychiatry, Zucker School of Medicine at Hofstra/Northwell, Hempstead, NY, USA.

Schizophrenia is associated with structural and functional changes in the central nervous system, including the most distal part of it: the retina. However, the question of whether retinal atrophy is present before individuals develop schizophrenia or is a secondary consequence of the disorder, caused for example, by pathophysiological processes or other confounders (e.g. antipsychotics) remains unanswered. We aimed to address this question by examining the association between polygenic risk scores for schizophrenia and retinal morphologies in individuals without a schizophrenia diagnosis. We used population data for white British and Irish individuals from the UK Biobank and estimated a polygenic risk score for schizophrenia based on the genome wide association data (PGC release 2022). We hypothesized that greater genetic susceptibility to schizophrenia is associated with thinner retinal tissue, specifically within the macula. To gain additional mechanistic insights, we conducted pathway-specific polygenic risk score associations analyses for gene pathways related to schizophrenia. Analyses were conducted for individual retinal layers as this provided the opportunity to distinguish between neurodevelopmental and neurodegenerative processes. Of 64283 individuals recruited, 34939 participants with available matching imaging-genetic data were included in the analysis, of whom 19070 (54.58%) were female and 15869 (45.42%) were male. According to our robust regression results, higher polygenic risk scores for schizophrenia were associated with thinner overall macular thickness while controlling for confounding factors ($b = -0.17$, $p = 0.018$). Similarly, we found that greater polygenic risk scores for schizophrenia specific to neuroinflammation gene sets were associated with thinner ganglion cell-inner plexiform layers ($b = -0.10$, self-contained $p = 0.014$; reflecting the level of association, competitive $p = 0.02$; reflecting the level of enrichment). These results provide new evidence for genetic factors that could predispose individuals to heightened neuroinflammatory responses. Over time these responses could contribute to progressive neurodegeneration, manifesting in part as retinal thinning. The results also suggest the involvement of inflammatory biomarkers in structural changes in the retina.

Introduction

Individuals with schizophrenia suffer from poor physical health and a reduced life expectancy. Poor physical health is reflected even in the most distal part of the central nervous system: the human retina. The retina is a direct extension of the brain that provides a non-invasive and real-time means of characterizing the neurovascular structure and function of the central nervous system.¹ Recent studies using optical coherence tomography found retinal thinning in individuals with schizophrenia.^{2–11} These studies have shown inner retinal atrophy, thinner peripapillary retinal nerve fiber layers and macular ganglion cell and inner plexiform layers, as well as an enlarged cup-disc ratio.

Findings such as these point to a neurobiological substrate of schizophrenia, detectable in this distal part of the central nervous system. However, in all of these studies the disorder was already present and it was thus unclear whether these differences in retinal thickness may have also been detectable at early stages, before the onset of symptoms. In addition, the presence of potentially confounding factors such as the effects of antipsychotic medication, smoking, lifestyle factors, and disease-related changes can impact retinal health. Such confounders can in turn obscure the interpretation of findings, making it difficult to determine whether observed differences in retinal thickness are directly related to the pathophysiology of schizophrenia or are secondary to these confounding factors.

Intriguingly, thinner retinas have been observed not only in patients but also in unaffected first-degree relatives, suggesting a link to genetic susceptibility to schizophrenia.³ Polygenic risk scores are an alternative to conventional heritability studies. They allow researchers to investigate the genetic underpinnings of retinal thickness differences in the context of schizophrenia risk, thus providing a potential understanding of the genetic contributions to retinal atrophy.¹² Polygenic risk scores aggregate the impact of numerous genetic variants throughout the genome and account for a considerable portion of the variance in disease risk.^{13,14} The identification of shared genetic influences between retinal structures and schizophrenia^{15,16} further supports the hypothesis that retinal atrophy observed in schizophrenia could re-

fect underlying genetic susceptibilities. This convergence from optical coherence tomography studies and genetic research may help in the exploration of the ways in which genetic predispositions contribute to the neurodevelopmental and neurodegenerative anomalies in schizophrenia¹⁷, including retinal alterations.

The present study asked whether thinner retinas are already detectable in healthy individuals with a higher genetic risk for schizophrenia. We focused on the macula, the area with the highest density of neurons in the retina (Fig. 1). Furthermore, we explored gene set-specific polygenic risk scores for schizophrenia: biological pathways that are related to neurotransmitter regulation, inflammation and microvasculature, all of which may be altered in individuals with schizophrenia.^{18–21} Pathway-specific analyses focused on the cumulative genetic risk within specific biological pathways, which may offer insights into the heterogeneity of the disease and its various manifestations.²² These analyses provide a more nuanced understanding of the genetic architecture of the disorder by exploring whether certain genetic pathways implicated in schizophrenia may also contribute to retinal thinning. This could help in elucidating the biological mechanisms underlying both the psychiatric and retinal manifestations of schizophrenia. To provide a more comprehensive understanding of how genetic risk affects different retinal structures, we not only focused on the inner retina (including the retinal nerve fiber layer, ganglion cell-inner plexiform layer and inner nuclear layer), but also the outer retina (inner nuclear layer - retinal pigment epithelium). If a certain pathway-related genetic risk for schizophrenia is associated with both higher genetic risk for schizophrenia and inner retinal thickness, this could indicate a shared biological basis that contributes to neurodegenerative processes. In summary, we hypothesized that higher polygenic risk for schizophrenia would be associated with a thinner macular tissue, and that this association would be reflected in pathways relevant for schizophrenia.

Methods

Base data: schizophrenia genome-wide association study (GWAS) 2022

The summary statistics base dataset was derived from the latest peer-reviewed genome-wide association study for schizophrenia.¹³ We used a file generated with the exclusion of samples from the UK Biobank to assure that the base and discovery files are independent. Following quality control (QC) recommendations¹⁴, we assured the same genome build with the discovery data (GRCh37/hg19), retained

Correspondence concerning this article should be addressed to Philipp Homan, MD, PhD, Department of Adult Psychiatry and Psychotherapy, University of Zurich, Lengstrasse 31, 8032 Zurich, Switzerland. E-mail: philipp.homan@bli.uzh.ch

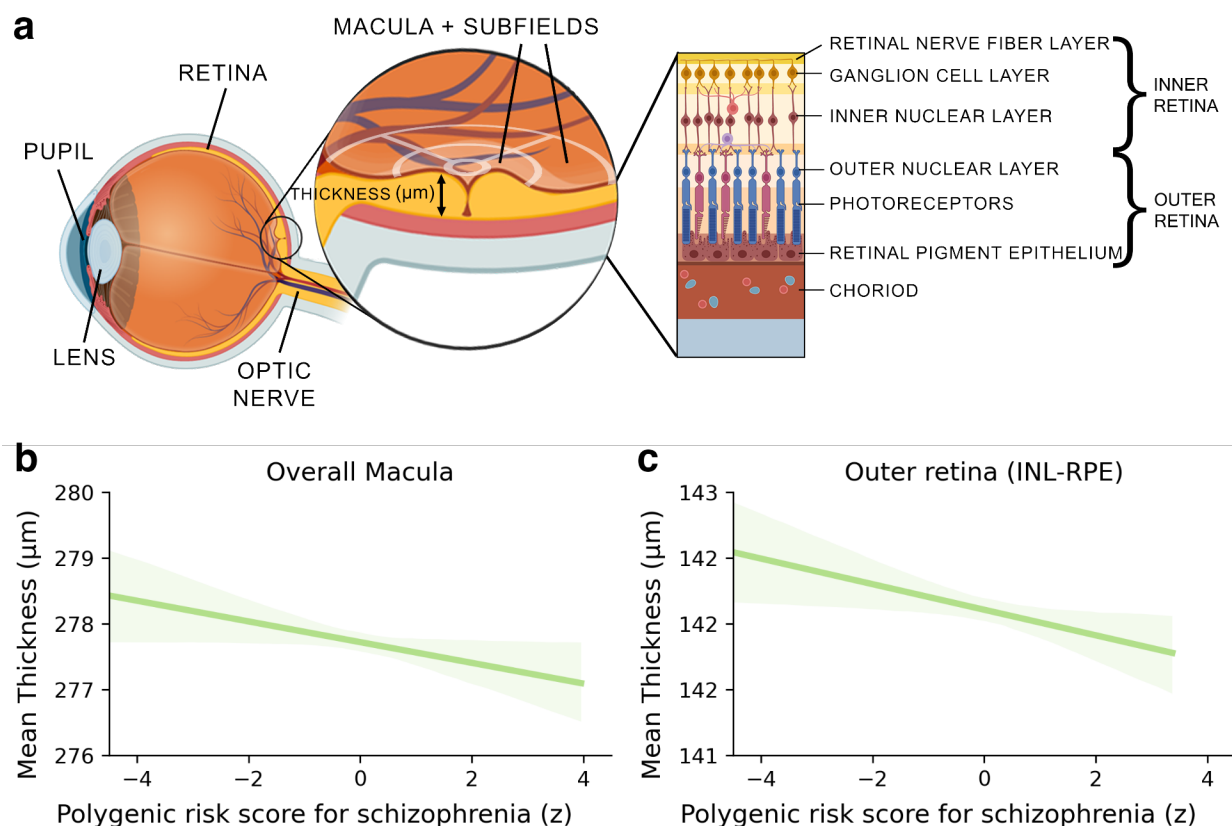


Figure 1. a. Anatomy of the eye and retina, displayed as cross section of the eye, and macular section of the retina. Optical coherence tomography measurements divide the macula in 9 subfields as indicated by white crosshairs. Macular thickness is measured in microns (micrometer). The structure of different layers of the inner and outer retina is displayed on the right. Association between polygenic risk scores (z-scored) for schizophrenia and (b) overall mean macular thickness (in micrometers) and (c) outer retinal thickness, averaged across both eyes. Solid lines represent the regression estimates, while complementary shaded areas correspond to 95 percent confidence intervals.

single-nucleotide polymorphisms (SNPs) with minor allele frequency $> 1\%$ and INFO score > 0.8 , checked for duplicate SNPs and removed ambiguous SNPs. The final base file included 5899135 SNPs.

Discovery data: UK Biobank genetic dataset

This study used data from the UK Biobank (application 102266). A full description of genotyping and imputation procedures of the UK Biobank data (<https://www.ukbiobank.ac.uk/>) is provided in the release documentation elsewhere.²³ Briefly, 487409 blood samples were assayed using two customized tagSNP arrays (the Applied Biosystems UK BiLEVE Axiom Array and the Applied Biosystems UK Biobank Axiom Array [Affymetrix, Santa Clara, CA, USA]) with 95% shared markers, imputed to the UK10K and 1000 Genome Project Phase 3 reference panels, with SHAPEIT3²⁴ used for phasing, and IMPUTE2²⁵ used for imputation. Further data handling and QC steps were carried out according to

a published processing pipeline.²⁶ To address population stratification, we retrieved ten genetic principal components from the UK Biobank. Specifically, after SNP extraction and alignment, conversion from bgen to PLINK format, removal of ambiguous SNPs (A/T, C/G; effects with allele frequencies between 0.4 and 0.6), data underwent a SNP-level QC (MAF < 0.005 and INFO score < 0.4) and sample-level QC (retaining individuals with missing rate in autosomes ≤ 0.02 , which were not outliers for genotype missingness or heterozygosity, not being genetically related to third-degree relatives, not being sex-discordant and of White British or Irish ethnicity according to genetic grouping). We also excluded all optical coherence tomography images with the worst 20% image quality and individuals with eye disorders and diseases known to affect the eye, including diabetes related eye diseases, glaucoma, macular degeneration, injury or trauma resulting in loss of vision. We also excluded individuals with

highly myopic and hyperopic eyes. Not only did we exclude all individuals that were “highly myopic” according to UK Biobank measurements and criteria²⁷, but we excluded extreme myopic ($SE \geq -6$ diopters) and hyperopic ($SE \leq 3$ diopters) eyes²⁸, as measured by a median spherical equivalent (SE) value for each eye. Finally, individuals with a ICD-10 diagnosis (F20 to F29), those who were medicated with antipsychotics, and those who had missing data for the variables of interest or covariates were excluded from any further analysis. A Little’s Missing Completely at Random (MCAR) test indicated that data were not MCAR ($p < .001$). Therefore, we used multiple imputation using predictive mean matching (PMM) to handle missing values and compared regression results between imputed and complete dataset. In total, $n = 34939$ individuals with matched imaging-genetic data were included in the final analysis (see Fig. 2 for details of participants’ inclusion and exclusion).

Polygenic risk scores calculations

In the main analysis, polygenic risk scores for schizophrenia were computed for each individual as a sum of risk alleles weighted by their estimated effect sizes²⁹ using the `-score` function in PLINK 2.0.³⁰ In addition, we generated five polygenic risk scores for schizophrenia for each individual, employing SNPs selected based on their significance in association with the phenotype in the discovery GWAS at nominal p-value thresholds of 0.01 or less, 0.05, 0.1, 0.5, and 1.00.

Derivation of pathway-based polygenic risk scores and signaling-pathway-specific analyses

We prioritized pathways known to be associated with the disease or phenotype of interest based on previous studies.^{18–21} Pathway polygenic risk scores were calculated by including only those SNPs that were relevant to the specific pathway under investigation and are also associated with schizophrenia. Pathway polygenic risk scores for schizophrenia were computed using PRSet¹⁴ in PRSice-2²⁹ for nine candidate gene sets selected from the Molecular Signatures Database version v2023.2 (<https://www.gsea-msigdb.org/>): acute inflammatory response (systematic name: M6557), TGF-beta signaling (M18933), chronic inflammatory response (M15140), positive regulation of dopamine receptor signaling pathway (M24111), Wnt signaling pathway involved in midbrain dopaminergic neuron differentiation (M25305), Wnt/beta-catenin pathways (M17761), neuroinflammatory response (M24927), abnormal retinal vascular morphology (M43559) and premature coronary artery atherosclerosis (M36658). For more details,

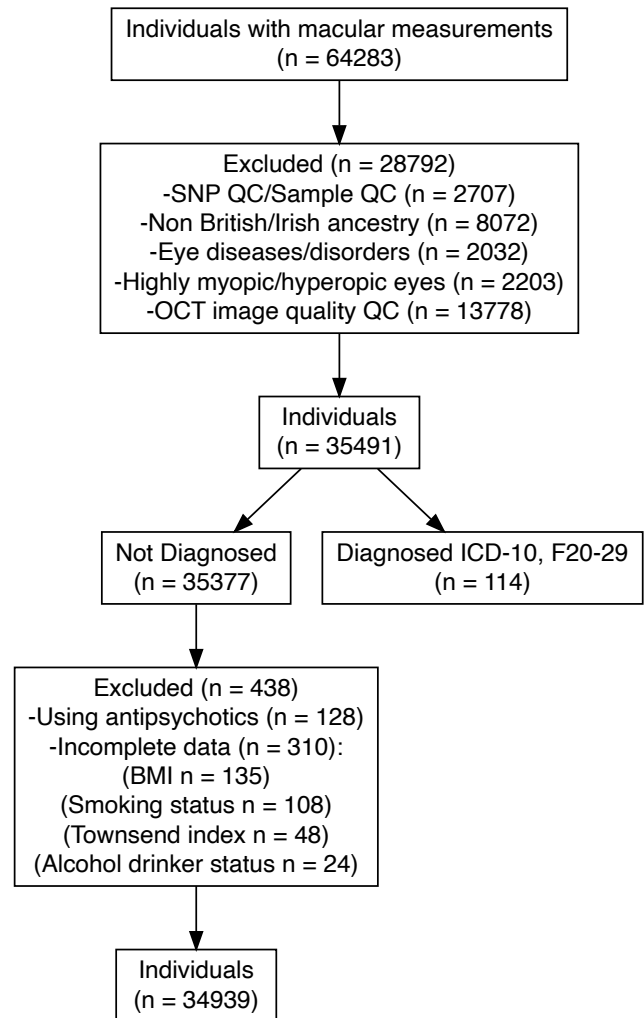


Figure 2. Diagram of inclusion and exclusion of participants in population. QC, Quality control; ICD, International Classification of Diseases; ICD-10, F20-29 categorization includes individuals with diagnosed schizophrenia, schizotypal and delusional disorders.

see *Gene pathways from the Molecular Signatures Database (MSigDB) version 7.4 utilized in pathway-based analysis* in the Supplementary Information. A PRSet p-value threshold was set at 1 due to the limited number of SNPs in gene-set polygenic risk scores, potentially not reflecting the entirety of gene sets accurately. Both the self-contained p-value and the competitive p-value were obtained. Self-contained methods tested each gene set independently to determine if the genes within the set were associated with the phenotype of interest. This approach does not compare the gene set to the rest of the genome. The level of association reflected by self-contained methods is the degree to which the genes within the pathway

are collectively associated with the phenotype, without considering genes outside the pathway.¹⁴ Competitive methods, on the other hand, compared the level of association between genes within a pathway and the rest of the genes in the genome. This approach tested whether the genes in the pathway are more associated with the phenotype than what would be expected by chance, given the level of association observed in genes outside the pathway. Thus, this competitive method reflected signal enrichment by determining if the pathway stood out against the genomic background.¹⁴ Both self-contained and competitive p-values were calculated within PRSet through 10,000 permutations to generate null distribution curves for p-values. The regression models consisted of thickness measures for retinal nerve fiber layer-, ganglion cell-inner plexiform layer-, inner nuclear layer-, outer retinal thickness and all covariates. Human GRCh37 genome version was used as the background file.

Optical coherence tomography protocol and analysis

Optical coherence tomography images were acquired between the years 2009 and 2010 using a spectral domain optical coherence tomography device, with a raster scan protocol of 6×6mm area centered on the fovea, consisting of 128 B-scans each with 512 A-scans, completed in 3.7 seconds. Automated analysis of retinal thickness was performed using custom software developed by Topcon Advanced Biomedical Imaging Laboratory, which used dual-scale gradient information for rapid segmentation of nine intraretinal boundaries, processing the images in approximately 120 seconds each. A comprehensive account of the standardized protocol employed for optical coherence tomography acquisition and the subsequent automated analysis of retinal thickness has previously been described.³¹ In the current study, we focused on the macula as it contains multiple layers that, based on prior investigations, show thinning in individuals diagnosed with schizophrenia.^{8,32,33}

Assessments of optical coherence tomography data distribution

The normality of the distribution for each retinal phenotype was assessed by visual inspection. However, the tailedness of the distributions for each retinal phenotype data appeared to be skewed by outliers (see diagonal in Fig. S2). We also computed the Pearson correlation coefficients between retinal phenotypes (Fig. S2).

Robust linear regression analysis for overall macular thickness and polygenic risk scores for schizophrenia

To account for potential outliers and heteroscedasticity observed in the retinal phenotype data, robust regression analysis was employed in order to examine the association between the polygenic risk scores for schizophrenia and macular phenotypes.

Robust linear regression employs M-estimation for robust linear modeling. M-estimators are a broad class of estimators in statistics that generalize maximum likelihood estimators, which are sensitive to outliers and violations of normality assumptions. The estimator used a Huber weight-function to downweight the influence of outliers and heavy-tailed distributions on the estimation of the model parameters.³⁴ We used the MASS::rlm package in R to conduct this robust analysis in which overall macular thickness was the dependent variable and polygenic risk scores for schizophrenia were the independent variable.

In this study when reporting b , we always refer to the standardized regression coefficient, which represents the estimated change in the dependent variable for a one-unit change in the independent variable.

Confounding factors

We included a comprehensive set of covariates in a multiple linear regression analysis for studying the association between polygenic risk scores for schizophrenia and macular thickness in isolation. These were age and quadratic age terms, genetic sex, hypertension diagnosed as ICD-10 (I10-15), diabetes mellitus diagnosed as ICD-10 (E10-14), alcohol drinker status, Body Mass Index (BMI), smoking status, Townsend Deprivation Index, optical coherence tomography image quality, the type of genotyping array used, and the first ten genetic principal components. The following rationale was applied for the inclusion of covariates: Age is a fundamental factor in the development of diseases, including macular changes and schizophrenia.³⁵ Various retinal structures are also known to degenerate with age.^{36,37} The inclusion of both linear and quadratic terms for age allows the model to capture not just a linear increase or decrease in risk or severity with age, but also any acceleration or deceleration in this trend. Furthermore, biological sex can influence the risk of developing various diseases, their progression, and response to treatment³⁸, and there is some evidence for sex differences in retinal structural parameters.³⁹ Hypertension can lead to hypertensive retinopathy which results in blurred vision, reduced vision, or even complete loss of sight if left untreated.⁴⁰ Likewise, di-

abetic retinopathy is a common microvascular complication of diabetes mellitus that can cause vision loss and blindness.⁴¹ Furthermore, alcohol consumption is associated with open-angle glaucoma.⁴²

Obesity is a well-known risk factor, as indicated by BMI, for a wide range of health conditions, and is associated in thinner retinal layer thickness.^{35,43} Similarly, smoking has been linked to an increased risk of various diseases, including those affecting the eyes.³⁸

The Townsend Deprivation Index in the UK Biobank reflects socioeconomic status, which can influence health outcomes, including those related to ophthalmic health.³⁸

The quality of optical coherence tomography images can influence the ability to detect macular changes.

Different genotyping arrays can have varying levels of accuracy or might target different sets of genetic variations and thus affect the computation of polygenic risk scores.⁴⁴ Likewise, the first ten genetic principal components account for population stratification, which can confound genetic associations. Including them in our models helps to ensure that any associations found are not due to underlying population genetic differences.³⁵

Statistical thresholding

Statistical significance for individual analyses was defined as $p < 0.05$. The pFWE significance threshold using the Holm-Bonferroni method was set at $p\text{FWE} < 0.1$.

Inflammatory biomarkers

The UK Biobank has meticulously recorded an array of inflammatory biomarkers between the years 2006 and 2010. Comprehensive details about their storage and analysis are available at the Biobank showcase. Peripheral blood cell counts, including lymphocyte, monocyte, neutrophil, and platelet counts, were obtained using an automated Coulter LH 750 analyzer. The instrument's differential blood cell count analysis provided calculated values for neutrophil, lymphocyte, and monocyte counts, with an operating range of $0.00\text{--}900.00 \times 10^9$ cells/L. Platelet counts were obtained directly from instrument measurements, with an operating range of $0.00\text{--}5000 \times 10^9$ cells/L. Using these peripheral blood cell counts, we derived four systemic inflammation markers: Systemic Immune-Inflammation Index (SII), Neutrophil-to-Lymphocyte Ratio (NLR), Platelet-to-Lymphocyte Ratio (PLR), and Lymphocyte-to-Monocyte Ratio (LMR). The calculations for these markers were as follows: $\text{SII} = (\text{neutrophils} \times \text{platelets}) / \text{lymphocytes}$, $\text{NLR} = \text{neutrophils} / \text{lymphocytes}$, $\text{PLR} = \text{platelets} / \text{lymphocytes}$, and $\text{LMR} = \text{lymphocytes} / \text{monocytes}$.⁴⁵ The measurement of serum C-reactive

protein (CRP) levels was carried out using a high-sensitivity immunoturbidimetric method on a Beckman Coulter AU5800 analyzer. In our analysis, we applied a logarithmic transformation to the CRP levels to address their notably skewed distribution, as illustrated in Fig. S3.

Partial effect analyses

In order to visualize individual phenotypes, we computed the correlation coefficients between the polygenic risk scores for schizophrenia and overall macular thickness while regressing out all confounding factors. Additionally, we extended this analysis to the combined thickness of outer retinal layers of the macula.

Mediation analysis

We further sought to elucidate the mechanisms underlying the association between a pathway-enriched polygenic risk score for schizophrenia, specifically the neuroinflammatory pathway, and inner and outer retinal thickness. Moreover, we investigated the potential mediating role of various inflammatory biomarkers in this relationship. The rationale for examining these markers as a mediator is grounded in the evidence linking neuroinflammatory processes to the pathophysiology of schizophrenia.^{46,47} Elevated levels of inflammatory biomarkers have been associated with increased risk and severity of schizophrenia, suggesting that inflammation may be a biological pathway through which genetic risk factors exert their effects on retinal phenotypes. To assess the mediation effect, we conducted a robust mediation analysis using two models. The mediator model was a robust linear regression that predicted inflammatory levels from neuroinflammatory-enriched polygenic risk for schizophrenia while controlling for before mentioned covariates. This model allowed us to estimate the effect of neuroinflammatory polygenic risk for schizophrenia on inflammatory biomarkers (Path A). The outcome model was another robust linear regression that predicted ganglion cell-inner plexiform layer thickness from both neuroinflammatory-specific polygenic risk for schizophrenia and markers, controlling for the same covariates. This model provided estimates for the direct effect of neuroinflammatory-specific polygenic risk for schizophrenia on retinal thickness (Path C) and the effect of inflammatory biomarkers on retinal thickness while accounting for neuroinflammatory-specific polygenic risk for schizophrenia (Path B).

The indirect effect ($\text{Path C}' = \text{Path A} * \text{Path B}$), representing the mediation effect of inflammatory biomarkers, was calculated as the product of the coefficients from Paths A and B. To evaluate the significance of the

effect, we employed a bootstrap method with 1000 re-samples, generating empirical confidence intervals for the mediation effect. This non-parametric approach allowed us to infer the robustness of the mediation effect without relying on the assumptions of normality. The p-value associated with this effect was computed through confidence interval inversion. Since fasting significantly reduces the number of circulating monocytes⁴⁸, we included fasting time as an additional covariate in this mediation analysis.

Data availability

All data utilized in this study is publicly available at the UK Biobank (<http://www.ukbiobank.ac.uk/>).

Code availability

All data analyses were performed between June 2023 and February 2024 using Python (version 3.9.12) and R (version 4.0.5). The manuscript was produced with the R packages rmarkdown (version 2.21)⁴⁹; MASS⁵⁰; SjPlot⁵¹; represearch (<https://github.com/phoman/represearch/>); kableExtra⁵²; knitr⁵³; papaja⁵⁴; matplotlib⁵⁵; seaborn⁵⁶; and scipy.⁵⁷ All code will be made freely available after publication to ensure reproducibility at <https://github.com/homanlab/prsoct/>.

Declaration of generative AI and AI-assisted technologies in the writing process

During the preparation of this work the authors used [OpenAI / GPT-4] in order to summarize their results. After using this tool, the authors reviewed and edited the content as needed and take full responsibility for the content of the publication.

Inclusion and Ethics Statement

This study utilized data from the UK Biobank, a large-scale biomedical database and research resource containing in-depth genetic and health information from half a million UK participants. Ethical approval for the use of UK Biobank data was obtained from the North West Multi-centre Research Ethics Committee (MREC). All participants provided informed consent, and data were anonymized to protect participant privacy. The research team adhered to the UK Biobank's policies on data access and usage, ensuring compliance with ethical standards and legal requirements. The study design and analysis were conducted with a commitment to inclusivity to ensure broad applicability of the findings.

Table 1
Sample characteristics

Characteristic	N	Mean (SD)
Female	19070	-
Male	15869	-
Diabetes Mellitus	19440	-
Hypertension	5204	-
Current smoker	3374	-
Previous smoker	12644	-
Non smoker	18921	-
Current alcohol drinker	32810	-
Previous alcohol drinker	1108	-
Non alcohol drinker	1021	-
Age	34939	56.87 (7.99)
BMI	34939	27.23 (4.67)
Townsend_index	34939	-1.36 (2.81)
Overall macular thickness (right)	34939	278.14 (20.37)
Overall macular thickness (left)	34939	275.69 (20.37)

Results

Overall reporting details

Out of the 64283 individuals recruited with available genetic and retinal data, 34939 individuals (54.40 %) were included for further analysis. Of these participants, 19070 (54.58 %) were females, and 15869 (45.42 %) were males (Table 1). We excluded 29344 individuals due to various QCs of genetic and optical coherence tomography data, eye diseases and disorders, the use of antipsychotic medications, and a diagnosis of ICD-10 (F20-F29). For more details, see Fig. 2. The linear regression models resulting from the analysis of the relationship between polygenic risk scores for schizophrenia and retinal phenotypes displayed heteroscedasticity. This was evidenced by all Breusch-Pagan tests yielding a chi-square statistic of $\chi^2 = 26.93$ with $p < .001$. This indicates that the variance of the residuals was not constant across the range of values, suggesting that the precision of the regression estimates varies depending on the level of the polygenic risk scores.

Polygenic risk for schizophrenia is associated with overall macular and outer retinal thickness

The primary dependent variable of the study was the retinal thickness at the macula. We conducted robust regression analyses to examine the relationships between polygenic risk scores for schizophrenia and mean macular thickness. We observed a negative relationship between macular thickness and polygenic risk scores for schizophrenia ($b = -0.17$, $CI = [-0.31, -0.03]$, $p = 0.018$; Figure 1b). This means that for each one standard deviation increase in polygenic risk for schizophrenia, the thickness of the macula decreased

by 0.17 micrometers. These robust regression results were similar to those obtained from the imputed dataset analysis ($b = -0.16$, $CI = [-0.30, -0.02]$, $p = 0.028$), suggesting the stability of the observed associations across different missing data handling approaches. Detailed association analysis results for left and right eye and their respective subfields can be viewed in the Supplementary Information (Fig. S1 and Table S2). Since the association between inner retinal thickness (specifically retinal nerve fiber layer, ganglion cell-inner plexiform layer, and inner nuclear layer) has been recently investigated⁵⁸, we extended our analysis to the outer retina. Strikingly, we also found a similar negative association for the outer retinal thickness ($b = -0.10$, $CI = [-0.18, -0.02]$, $p = 0.018$, $pFWER = 0.04$; Fig. 1c). For robust regression results for the inner and outer retina, see Table S1.

Neuroinflammatory pathway-specific polygenic risk scores are associated with thicknesses of specific layers in the inner retina

Pathway-specific polygenic risk scores are crucial for association analysis with retinal thickness because they allowed us to pinpoint specific biological mechanisms underlying the observed retinal changes in schizophrenia patients. Intriguingly, we observed that higher polygenic risk scores specific to neuroinflammation in relation to schizophrenia were significantly associated with thinner ganglion cell-inner plexiform layers ($b = -0.10$, self-contained $p = 0.014$, competitive $p = 0.023$) (Table 2). We found no statistically significant associations with other gene pathways that potentially could be related to schizophrenia (for more details, see Table S4).

C-reactive protein levels partially mediate the association between neuroinflammatory pathway-specific polygenic risk for schizophrenia and retinal thickness

The UK Biobank also provided us with inflammatory marker measurements, which play a pivotal role in managing inflammation. Therefore, we explored the mediating role of these markers in the relationship between neuroinflammatory-enriched polygenic risk scores for schizophrenia and ganglion cell-inner plexiform layer as an outcome variable (Table 3). The mediator model revealed a significant effect of neuroinflammatory-specific polygenic risk scores for schizophrenia on CRP (Path A coefficient = 0.01), controlling for confounding factors. This positive correlation between neuroinflammation gene enriched polygenic risk scores for schizophrenia and CRP levels suggests that individuals with a higher genetic risk

Table 2

*Association between polygenic risk for schizophrenia enriched for multiple gene pathways and inner and outer retinal thickness at p-value threshold 1. Microvasculature pathways: 1. Human phenotype (HP) abnormal retinal vascular morphology (M43559) 2. HP premature coronary artery atherosclerosis (M36658). Inflammatory pathways: 1. Gene Ontology Biological Process (GOBP) acute inflammatory response (M6557) 2. GOBP neuroinflammatory response (M24927) 3. Biocarta TGFB pathway (M18933) 4. GOBP chronic inflammatory response (M15140). Signaling pathways influencing neuronal development: 1. GOBP Wnt signaling pathway involved in midbrain dopaminergic neuron differentiation (M25305) 2. GOBP positive regulation of dopamine receptor signaling pathway (M24111) 3. ST Wnt beta catenin pathway (M17761). Standard errors in brackets. * $p < 0.05$, ** $p < 0.01$. RNFL, Retinal nerve fiber layer; GCIPL, Ganglion cell layer to inner plexiform layer; INL, Inner nuclear layer; INLRPE, Inner nuclear layer to retinal pigment epithelium.*

GeseaPathwayCode	RNFL	GCIPL	INL	INLRPE
M43559	0.02 (0.03)	-0.02 (0.04)	0.00 (0.02)	-0.02 (0.06)
M6557	0.04 (0.03)	-0.05 (0.04)	0.02 (0.02)	-0.09 (0.06)
M17761	-0.03 (0.03)	-0.06 (0.04)	-0.02 (0.02)	-0.00 (0.06)
M15140	0.04 (0.03)	0.01 (0.04)	0.00 (0.02)	-0.07 (0.06)
M36658	-0.02 (0.03)	0.00 (0.04)	0.01 (0.02)	0.04 (0.06)
M24111	0.03 (0.03)	0.01 (0.04)	-0.01 (0.02)	-0.01 (0.06)
M24927	-0.02 (0.03)	-0.10* (0.04)	-0.01 (0.02)	-0.01 (0.07)
M18933	0.01 (0.03)	-0.05 (0.04)	0.02 (0.02)	-0.09 (0.06)
M25305	-0.03 (0.03)	-0.03 (0.04)	0.02 (0.02)	-0.01 (0.07)

* $p < 0.05$

for schizophrenia, particularly in genes related to neuroinflammation, tend to exhibit elevated levels of systemic inflammation, as measured by CRP concentrations. Furthermore, the outcome model showed a significant effect of CRP on ganglion cell-inner plexiform layer thickness, after accounting for the same covariates, fasting time, and neuroinflammatory polygenic risk for schizophrenia. The estimated indirect effect of neuroinflammatory-specific polygenic risk for schizophrenia on ganglion cell-inner plexiform layer through the mediator CRP was -0.001, with a 95% bootstrap confidence interval of $[-0.003, -0.0002]$, suggesting a statistically significant partial mediation effect ($p = 0.030$). This means that part of the negative impact of neuroinflammatory-specific polygenic risk scores for schizophrenia on ganglion cell-inner plexiform layer is mediated by increased CRP levels. More specifically, approximately 1.28% of the total effect of neuroinflammatory-specific polygenic risk scores for schizophrenia on retinal thickness is mediated by CRP levels. This result indicates that while CRP does play a statistically significant role in mediating the relationship between genetic risk for schizophrenia and retinal thinning, its contribution is relatively small. The majority of

the effect (about 98.72%) is likely due to direct effects or other mediating factors not captured by CRP levels alone. For all other inflammatory markers we did not find such a mediation effect.

Table 3

*Mediation effects of inflammatory marker on the association between neuroinflammatory-specific polygenic risk for schizophrenia and ganglion cell-inner plexiform layer thickness. SII, Systemic Immune-Inflammation Index; NLR, Neutrophil-to-Lymphocyte Ratio; PLR, Platelet-to-Lymphocyte Ratio; LMR, Lymphocyte-to-Monocyte Ratio; CRP, C-reactive protein levels; * = $p < 0.05$, ** = $p < 0.01$, *** = $p < 0.001$*

	SII	NLR	PLR	LMR	CRP
Path A	-1.7 [-4.1, 0.76]	-0.01 [-0.01, 0]	-0.2 [-0.65, 0.24]	0 [-0.02, 0.01]	0.01* [0, 0.02]
Path B	0 [0, 0]	-0.01 [-0.05, 0.04]	0 [0, 0]	0.02 [0, 0.04]	-0.09* [-0.16, -0.03]
Total Effect	-0.09*** [-0.15, -0.03]	-0.09*** [-0.15, -0.03]	-0.09*** [-0.15, -0.03]	-0.09*** [-0.15, -0.03]	-0.09*** [-0.15, -0.03]
Direct Effect	-0.09*** [-0.15, -0.03]	-0.09*** [-0.15, -0.03]	-0.09*** [-0.15, -0.03]	-0.09*** [-0.15, -0.03]	-0.09*** [-0.15, -0.03]
Indirect Effect	0 [-0.001, 0]	0 [0, 0]	0 [-0.001, 0]	0 [-0.001, 0]	-0.001* [-0.003, 0]

Discussion

In this large observational study in healthy individuals, we found that an increased genetic risk for schizophrenia is associated with lower retinal thickness. This demonstrates that schizophrenia's genetic risk factors affect not just the brain but also the retina. This result reaffirms the findings of a recent study of the genetic contribution to retinal thickness within the context of schizophrenia risk⁵⁸, in which it was found that, using inner retina-specific analyses, higher genetic risk for schizophrenia is associated with thinner ganglion cell-inner plexiform layers. Our results extend these findings by providing evidence that greater genetic risk for schizophrenia is also associated with thinner outer retinal thickness. This presents a more complete picture on the connection between genetic risk and retinal morphology.

What are the exact mechanisms underlying these retinal alterations in individuals with greater genetic risk for schizophrenia? We provide a potential explanation whereby the expression or activity of a set of genes may trigger neuroinflammatory cascades that affect retinal structure, resulting in measurable changes to the thickness of the ganglion cell-inner plexiform layer.

This finding holds great importance as it provides a unique window into the neurobiological underpinnings

of schizophrenia, potentially revealing early markers of disease risk and progression.

Inflammatory processes can disrupt the normal functioning of astrocytes, potentially leading to neurotransmitter dysregulation and blood–brain barrier permeability.^{59,60} Blood-brain barrier disruption, caused by pro-inflammatory cytokines and chemokines, can exacerbate neuroinflammation by allowing immune cells and potentially harmful substances to enter the brain.^{59,61} This can lead to the release of acute-phase proteins, oxidative stress, excitotoxicity, and other processes that cause neuronal damage. This in turn affects synaptic functioning, which is critical for normal cognitive processes and has been found to be disrupted in schizophrenia.^{59,61} Acute-phase proteins like CRP can also contribute to the progressive apoptosis of photoreceptors.^{62,63} This might explain our finding of a partial mediation effect of CRP, suggesting its mediating role next to other potential candidates, on the association between neuroinflammatory enriched polygenic risk scores for schizophrenia and retinal thickness. In the case that CRP does serve a mediating role, this would suggest that neuroinflammatory processes, as indexed by CRP levels, could be a key biological pathway through which genetic risk factors for schizophrenia contribute to macular effects. While a previous study found no association between the levels of inflammatory markers (CRP among others) and retinal thickness in either the schizophrenia or control group⁶⁴, that study was considerably smaller than the present study. It is possible that such an effect can only be detected with substantially more statistical power, coming from a large sample size as in our study.

Intriguingly, the fact that CRP mediation affects the ganglion cell-inner plexiform layer suggests that the inflammatory processes associated with schizophrenia risk may have selective effects throughout the retina, presumably targeting amacrine cells in that layer.¹⁰ By examining differential effects on retinal layers, we gained insights into specific cellular and molecular pathways implicated in the disorder, which may lead to the development of more targeted therapeutic interventions.

We also explored more genetic pathways that may contribute to retinal effects in individuals with increasing polygenic risk for schizophrenia. For instance, Wnt signaling pathways could play a significant role in the protection of damaged retinal neurons.^{19,65,66} They have been shown to have a significant impact on retinal vessel formation and maturation, as well as on the establishment of synaptic structures and neuronal function in the central nervous system.⁶⁵ The activation of certain Wnt pathways has been shown to reverse the patho-

logical phenotype caused by Wnt inhibition in the context of glaucoma.⁶⁷ However, in the case of the present study, neither of the Wnt signaling pathways showed a significant association with macular thickness changes. This could be because our selection of these pathways was very limited and/or the gene sets of these pathways did not fully capture the polygenic nature of the effects.

In summary, the genetic risk factors for schizophrenia, as represented by the polygenic risk scores, may influence neuroinflammatory pathways involved in the disease. These pathways could, in turn, affect the neural and vascular integrity of the retina, leading to observable retinal changes. While we observed a relationship between polygenic risk scores and retinal layer thickness at the macula, we did not observe any associations between retinal microvasculature gene-based polygenic risk scores for schizophrenia and retinal phenotypes. This could be due to the fact that genetic architecture of retinal microvasculature traits and schizophrenia risk is complex and again, the selected pathways were not able to capture this relationship. Alternatively, retinal thickness in individuals with high polygenic risk for schizophrenia may also be influenced by other factors e.g. systemic comorbidities like metabolic dysfunction, certain health behaviors, and life-course exposures, which were not evaluated in this study. Future investigations should explore potential gene-environment interactions. For example, given the known effects of smoking on retinal inflammation and ocular health^{68,69}, research should examine whether there is an interaction between PRS for schizophrenia, smoking, and retinal thinning. Such research could provide valuable insights into how lifestyle factors may accelerate neurodegeneration in genetically predisposed individuals.⁷⁰

Several limitations merit comment. The UK Biobank sample is not fully representative of the UK population, due to its low response rate, under-representation of younger individuals and socioeconomically deprived areas, and lower prevalence of certain health conditions like schizophrenia. Our study focused on participants of British or Irish descent, as they constituted the majority of the available data. All of this limits our results in their generalizability to a wider population. Moreover, while robust regression provides advantages in handling outliers and heteroscedasticity, it is crucial to interpret the results in the context of the method's characteristics. The downweighting of extreme observations might dilute extreme but genuine phenomena. We would also like to note that the temporal disparity in data collection introduced potential unmeasured confounding factors, such as lifestyle changes, medical interventions,

or environmental influences, which could independently affect inflammatory marker levels or retinal measurements. Finally, the polygenic risk score's explanatory power for schizophrenia is modest, which may have limited the detection of small effects. A $-0.17\ \mu\text{m}$ change represents only about 0.065% of the average overall macular thickness. This extremely small variation is very unlikely to have an impact on visual acuity, given previous evidence that a much larger change in retinal thickness was associated with only a minimal change in visual acuity.⁷¹

Our study also had several strengths, including the use of a large, population-based sample from the UK Biobank, which allowed us to avoid confounding factors related to psychotic and retinal abnormalities or antipsychotic use. We also employed robust statistical analyses and complementary techniques to enhance the reliability of our results. Additionally, our extended analyses produced consistent findings across multiple inclusion thresholds for the polygenic risk score. Our study further benefits from the establishment of temporal precedence in the mediation analysis, as inflammatory biomarkers were measured before retinal thickness outcomes, strengthening the causal interpretation of our findings.⁷²

In conclusion, our study identified significant associations between polygenic risk scores for schizophrenia, pathway-specific scores, and specific retinal layers, offering valuable insights into the genetic contributions to retinal changes in individuals without any diagnosis of schizophrenia. These findings suggest that the retina may serve not only as a "window" into the brain but also as a mirror reflecting the genetic complexities of schizophrenia. They allow us to better distinguish between primary effects of genetic risk and secondary consequences of the disorder. While our results increase confidence that retinal thinning may be associated with core processes in schizophrenia, further research is crucial to establish the specificity and sensitivity of retinal thinning as a reliable indicator of core degenerative processes in the disorder. Future studies should focus on disentangling the complex interplay between genetic predisposition, environmental factors, and comorbid conditions that can affect retinal health, to determine the true potential of retinal changes as a biomarker for schizophrenia-related processes.

Acknowledgements

Figures 1a and 1c include graphics created with BioRender.com.

Role of the funding source

PH is supported by a NARSAD grant from the Brain & Behavior Research Foundation (28445) and by a Research Grant from the Novartis Foundation (20A058). The study design, data collection, data analysis, data interpretation, and report writing was conducted independently, without involvement from the funders.

T.L. was supported by the National Institute of Mental Health of the National Institutes of Health (NIH) under award no. R01MH117646 (T.L., principal investigator). The content is solely the responsibility of the authors and does not necessarily represent the official views of the NIH.

Competing interests

PH has received grants and honoraria from Novartis, Lundbeck, Mepha, Janssen, Boehringer Ingelheim, Neurolite outside of this work. No other disclosures were reported.

Author contributions

FR: conceptualization, methodology, statistical analysis, visualization, writing, review and editing. LK: methodology, genetic analysis, writing, review and editing. FG: conceptualization, methodology and statistical analysis. NK: conceptualization and supervision. WO: review and editing. VE: review and editing. MK: review and editing. FC: review and editing. EG: methodology, review and editing. SS: supervision, review & editing. BB: review & editing. DB: review & editing. KS: review & editing. JR: review & editing. TL: supervision, methodology, review & editing. PH: supervision, conceptualization, writing, review and editing.

References

1. London, A., Benhar, I. & Schwartz, M. The retina as a window to the brain—from eye research to CNS disorders. *Nature Reviews Neurology* **9**, 44–53 (2012).
2. Lee, W. W., Tajunisah, I., Sharmilla, K., Peyman, M. & Subrayan, V. Retinal nerve fiber layer structure abnormalities in schizophrenia and its relationship to disease state: Evidence from optical coherence tomography. *Investigative Ophthalmology & Visual Science* **54**, 7785 (2013).
3. Asanad, S. *et al.* Neuroretinal biomarkers for schizophrenia spectrum disorders. *Translational Vision Science & Technology* **10**, 29 (2021).
4. Gonzalez-Diaz, J. M. *et al.* Mapping retinal abnormalities in psychosis: Meta-analytical evidence for focal peripapillary and macular reductions. *Schizophrenia Bulletin* **48**, 1194–1205 (2022).
5. Komatsu, H. *et al.* Retinal layers and associated clinical factors in schizophrenia spectrum disorders: A systematic review and meta-analysis. *Molecular Psychiatry* **27**, 3592–3616 (2022).
6. Friedel, E. B. N. *et al.* Structural and functional retinal alterations in patients with paranoid schizophrenia. *Translational Psychiatry* **12**, (2022).
7. Boudriot, E. *et al.* Optical coherence tomography reveals retinal thinning in schizophrenia spectrum disorders. *European Archives of Psychiatry and Clinical Neuroscience* **273**, 575–588 (2022).
8. Wagner, S. K. *et al.* Association between retinal features from multimodal imaging and schizophrenia. *JAMA Psychiatry* **80**, 478 (2023).
9. Shew, W., Zhang, D. J., Menkes, D. B. & Danesh-Meyer, H. V. Optical coherence tomography in schizophrenia spectrum disorders: A systematic review and meta-analysis. *Biological Psychiatry Global Open Science* **4**, 19–30 (2024).
10. Boudriot, E. *et al.* Genetic analysis of retinal cell types reveals synaptic pathology in schizophrenia. *bioRxiv* (2024) doi:10.1101/2024.08.09.607343.
11. Kallen, N. M. *et al.* The retina across the psychiatric spectrum: A systematic review and meta-analysis. *medRxiv* (2024) doi:10.1101/2024.11.07.24316925.
12. Henriksen, M. G., Nordgaard, J. & Jansson, L. B. Genetics of schizophrenia: Overview of methods, findings and limitations. *Frontiers in Human Neuroscience* **11**, (2017).
13. Trubetskoy, V. *et al.* Mapping genomic loci implicates genes and synaptic biology in schizophrenia. *Nature* **604**, 502–508 (2022).
14. Choi, S. W., Mak, T. S.-H. & O'Reilly, P. F. Tutorial: A guide to performing polygenic risk score analyses. *Nature Protocols* **15**, 2759–2772 (2020).
15. Zhao, B. *et al.* Eye-brain connections revealed by multimodal retinal and brain imaging genetics in the UK biobank. *medRxiv* (2023) doi:10.1101/2023.02.16.23286035.

16. Lazzerini Ospri, L. *et al.* Light affects the prefrontal cortex via intrinsically photosensitive retinal ganglion cells. *Science Advances* **10**, (2024).
17. Schor, N. F. & Bianchi, D. W. Neurodevelopmental clues to neurodegeneration. *Pediatric Neurology* **123**, 67–76 (2021).
18. Kirkpatrick, B. & Miller, B. J. Inflammation and schizophrenia. *Schizophrenia Bulletin* **39**, 1174–1179 (2013).
19. Vallee, A. Neuroinflammation in schizophrenia: The key role of the WNT/beta-catenin pathway. *International Journal of Molecular Sciences* **23**, 2810 (2022).
20. Silverstein, S. M. *et al.* Retinal microvasculature in schizophrenia. *Eye and Brain* **Volume 13**, 205–217 (2021).
21. Luvsannyam, E. *et al.* Neurobiology of schizophrenia: A comprehensive review. *Cureus* (2022) doi:10.7759/cureus.23959.
22. Touloupoulou, T. *et al.* Polygenic risk score increases schizophrenia liability through cognition-relevant pathways. *Brain* **142**, 471–485 (2018).
23. Bycroft, C. *et al.* The UK biobank resource with deep phenotyping and genomic data. *Nature* **562**, 203–209 (2018).
24. O'Connell, J. *et al.* Haplotype estimation for biobank-scale data sets. *Nature Genetics* **48**, 817–820 (2016).
25. Howie, B. N., Donnelly, P. & Marchini, J. A flexible and accurate genotype imputation method for the next generation of genome-wide association studies. *PLoS Genetics* **5**, e1000529 (2009).
26. Collister, J. A., Liu, X. & Clifton, L. Calculating polygenic risk scores (PRS) in UK biobank: A practical guide for epidemiologists. *Frontiers in Genetics* **13**, (2022).
27. Guggenheim, J. A. & Williams, C. Role of educational exposure in the association between myopia and birth order. *JAMA Ophthalmology* **133**, 1408 (2015).
28. Group, T. E. D. P. R. The prevalence of refractive errors among adults in the united states, western europe, and australia. *Archives of Ophthalmology* **122**, 495–505 (2004).
29. Choi, S. W. & O'Reilly, P. F. PRSice-2: Polygenic risk score software for biobank-scale data. *GigaScience* **8**, (2019).
30. Chang, C. C. *et al.* Second-generation PLINK: Rising to the challenge of larger and richer datasets. *GigaScience* **4**, (2015).
31. Keane, P. A. *et al.* Optical coherence tomography in the UK biobank study – rapid automated analysis of retinal thickness for large population-based studies. *PLOS ONE* **11**, e0164095 (2016).
32. Kazakos, C. T. & Karageorgiou, V. Retinal changes in schizophrenia: A systematic review and meta-analysis based on individual participant data. *Schizophrenia Bulletin* (2019) doi:10.1093/schbul/sbz106.
33. Komatsu, H. *et al.* Retina as a potential biomarker in schizophrenia spectrum disorders: A systematic review and meta-analysis of optical coherence tomography and electroretinography. *Molecular Psychiatry* (2023) doi:10.1038/s41380-023-02340-4.
34. Huber, P. J. *Robust statistics*. (John Wiley & Sons, Inc., 1981). doi:10.1002/0471725250.
35. Wąsowska, A. *et al.* Polygenic risk score impact on susceptibility to age-related macular degeneration in polish patients. *Journal of Clinical Medicine* **12**, 295 (2022).
36. Wei, Y. *et al.* Age-related alterations in the retinal microvasculature, microcirculation, and microstructure. *Investigative Ophthalmology & Visual Science* **58**, 3804 (2017).
37. Georgiadis, F. *et al.* Detecting accelerated retinal decline in mental disorders through normative modeling. *medRxiv* (2024) doi:10.1101/2024.06.11.24308654.
38. Zekavat, S. M. *et al.* Insights into human health from phenome- and genome-wide analyses of UK biobank retinal optical coherence tomography phenotypes. *medRxiv* (2023) doi:10.1101/2023.05.16.23290063.
39. Ryoo, N.-K. *et al.* Thickness of retina and choroid in the elderly population and its association with complement factor h polymorphism: KLoSHA eye study. *PLOS ONE* **13**, e0209276 (2018).
40. Dziedziak, J., Zaleska-Żmijewska, A., Szaflik, J. P. & Cudnoch-Jędrzejewska, A. Impact of arterial hypertension on the eye: A review of the pathogenesis, diagnostic methods, and treatment of hypertensive retinopathy. *Medical Science Monitor* **28**, (2022).

41. Wang, W. & Lo, A. C. Y. Diabetic retinopathy: Pathophysiology and treatments. *International Journal of Molecular Sciences* **19**, 1816 (2018).
42. Grant, A. *et al.* Alcohol consumption, genetic risk, and intraocular pressure and glaucoma: The canadian longitudinal study on aging. *Investigative Ophthalmology & Visual Science* **64**, 3 (2023).
43. Laiginhas, R. *et al.* Retinal nerve fiber layer thickness decrease in obesity as a marker of neurodegeneration. *Obesity Surgery* **29**, 2174–2179 (2019).
44. Verlouw, J. A. M. *et al.* A comparison of genotyping arrays. *European Journal of Human Genetics* **29**, 1611–1624 (2021).
45. Nøst, T. H. *et al.* Systemic inflammation markers and cancer incidence in the UK biobank. *European Journal of Epidemiology* **36**, 841–848 (2021).
46. Fond, G., Lançon, C., Auquier, P. & Boyer, L. C-reactive protein as a peripheral biomarker in schizophrenia. An updated systematic review. *Frontiers in Psychiatry* **9**, (2018).
47. Prins, Bram. P. *et al.* Investigating the causal relationship of c-reactive protein with 32 complex somatic and psychiatric outcomes: A large-scale cross-consortium mendelian randomization study. *PLOS Medicine* **13**, e1001976 (2016).
48. Jordan, S. *et al.* Dietary intake regulates the circulating inflammatory monocyte pool. *Cell* **178**, 1102–1114.e17 (2019).
49. Allaire, J. *et al.* Rmarkdown: Dynamic documents for r. *CRAN: Contributed Packages* (2014) doi:10.32614/cran.package.rmarkdown.
50. Ripley, B. & Venables, B. MASS: Support functions and datasets for venables and ripley's MASS. *CRAN: Contributed Packages* (2009) doi:10.32614/cran.package.mass.
51. Lüdecke, D. sjPlot: Data visualization for statistics in social science. *CRAN: Contributed Packages* (2013) doi:10.32614/cran.package.sjplot.
52. Zhu, H. kableExtra: Construct complex table with 'kable' and pipe syntax. *CRAN: Contributed Packages* (2017) doi:10.32614/cran.package.kableextra.
53. Xie, Y. Knitr: A general-purpose package for dynamic report generation in r. *CRAN: Contributed Packages* (2012) doi:10.32614/cran.package.knitr.
54. Aust, F. & Barth, M. Papaja: Prepare american psychological association journal articles with r markdown. *CRAN: Contributed Packages* (2022) doi:10.32614/cran.package.papaja.
55. Hunter, J. D. Matplotlib: A 2D graphics environment. *Computing in Science & Engineering* **9**, 90–95 (2007).
56. Waskom, M. Seaborn: Statistical data visualization. *Journal of Open Source Software* **6**, 3021 (2021).
57. Virtanen, P. *et al.* SciPy 1.0: Fundamental algorithms for scientific computing in python. *Nature Methods* **17**, 261–272 (2020).
58. Blose, B. A. *et al.* Association between polygenic risk for schizophrenia and retinal morphology: A cross-sectional analysis of the united kingdom biobank. *Psychiatry Research* **339**, 116106 (2024).
59. Pan, J. *et al.* Age-associated changes in microglia and astrocytes ameliorate blood-brain barrier dysfunction. *Molecular Therapy - Nucleic Acids* **26**, 970–986 (2021).
60. Cruz, J. V. R., Batista, C., Diniz, L. P. & Mendes, F. A. The role of astrocytes and blood-brain barrier disruption in alzheimer's disease. *Neuroglia* **4**, 209–221 (2023).
61. Gullotta, G. S., Costantino, G., Sortino, M. A. & Spampinato, S. F. Microglia and the blood-brain barrier: An external player in acute and chronic neuroinflammatory conditions. *International Journal of Molecular Sciences* **24**, 9144 (2023).
62. Kaur, G. & Singh, N. K. The role of inflammation in retinal neurodegeneration and degenerative diseases. *International Journal of Molecular Sciences* **23**, 386 (2021).
63. Noailles, A. *et al.* Persistent inflammatory state after photoreceptor loss in an animal model of retinal degeneration. *Scientific Reports* **6**, (2016).
64. Carriello, M. A. *et al.* Retinal layers and symptoms and inflammation in schizophrenia. *European Archives of Psychiatry and Clinical Neuroscience* (2023) doi:10.1007/s00406-023-01583-0.
65. Ohlmann, A., Kassemeh, S., Weber, G., Nobl, M. & Priglinger, S. The neuroprotective role of wnt signaling in the retina. *Neural Regeneration Research* **16**, 1524 (2021).

66. Zhuang, W., Ye, T., Wang, W., Song, W. & Tan, T. CTNNB1 in neurodevelopmental disorders. *Frontiers in Psychiatry* **14**, (2023).
67. Dhamodaran, K., Baidouri, H., Sandoval, L. & Raghunathan, V. Wnt activation after inhibition restores trabecular meshwork cells toward a normal phenotype. *Investigative Ophthalmology & Visual Science* **61**, 30 (2020).
68. Oishi, A. *et al.* Effect of smoking on macular function and retinal structure in retinitis pigmentosa. *Brain Communications* **2**, (2020).
69. Wang, F. *et al.* Retinal tissue develops an inflammatory reaction to tobacco smoke and electronic cigarette vapor in mice. *Journal of Molecular Medicine* **99**, 1459–1469 (2021).
70. Koster, M. *et al.* The association between chronic tobacco smoking and brain alterations in schizophrenia: A systematic review of magnetic resonance imaging studies. *Schizophrenia Bulletin* (2024) doi:10.1093/schbul/sbae088.
71. Lee, S. S.-Y. *et al.* Macular thickness profile and its association with best-corrected visual acuity in healthy young adults. *Translational Vision Science & Technology* **10**, 8 (2021).
72. Mendelson, D., Mizrahi, R., Lepage, M. & Lavigne, K. M. C-reactive protein and cognition: Mediation analyses with brain morphology in the UK biobank. *Brain, Behavior, & Immunity - Health* **31**, 100664 (2023).

Supplementary Results

HP_ABNORMAL_RETINAL_VASCULAR_MORPHOLOGY > An identifier suggests a phenotype related to abnormal morphology (structure) of the blood vessels in the retina. [ABCA4 ABCC6 ACVRL1 AGBL5 AHI1 AHR AIPL1 ANTXR1 APOC2 ARHGEF18 ARL2BP ARL3 ARL6 ARV1 ARVCF ASAH1 ATF6 BAZ1B BBS1 BBS2 BBS9 BCL7B BEST1 BUD23 CA4 CAPN5 CC2D2A CCDC28B CCM2 CCND1 CDHR1 CENPF CERKL CFAP410 CFAP418 CHM CLCC1 CLCNKB CLIP2 CLRN1 CNGA1 CNGA3 CNGB1 CNGB3 CNNM4 COL18A1 COL4A1 COMT CRB1 CRX CTC1 CTNNB1 CTSA CYP1B1 CYP27A1 DARS1 DGCR2 DGCR6 DGCR8 DHDDS DHX38 DLK1 DLST DNAJC30 DNMT3A DNMT3B DUX4 DUX4L1 EFEMP1 EIF4H ELN ENG ENPP1 EPAS1 ERCC4 ESS2 ETHE1 EYS F12 FAM161A FGF12 FH FKBP6 FLVCR1 FRG1 FSCN2 FUCA1 FZD4 G6PC1 GALC GDF2 GGCX GLB1 GM2A GNAQ GNAT2 GP1BB GPIHBP1 GTF2I GTF2IRD1 GTF2IRD2 GUCA1B GUCY2D HARS1 HEXA HEXB HGSNAT HIRA HK1 HLA-A HSD11B2 IDH3A IDH3B IFT140 IFT172 IFT43 IFT88 IGFBP7 IKBKG IMPDH1 IMPG1 IMPG2

IVNS1ABP JMJD1C KIAA1549 KIF1B KIZ KLHL7 KRIT1 LAMB2 LCA5
LCK LIMK1 LOXL1 LPL LRAT LRP5 LRRC32 MAK MAX MDH2 MEG3
MERTK METTL27 MKS1 MLXIPL MT-ATP6 MT-CO1 MT-CO3 MT-CYB
MT-ND1 MT-ND2 MT-ND4 MT-ND4L MT-ND5 MT-ND6 MVK MYD88
MYOC NCF1 NDP NDUFS2 NEK1 NEK2 NEU1 NF1 NMNAT1 NOD2
NR2E3 NRL NUS1 OFD1 PAX6 PCARE PCNA PDCD10 PDE6A PDE6B
PDE6C PDE6G PDE6H PIK3CA POMGNT1 PRCD PROM1 PRPF3 PRPF31
PRPF4 PRPF6 PRPF8 PRPH2 PSAP RAX2 RBP3 RDH11 RDH12 RDH5
REEP6 RET RFC2 RGR RHO RLBP1 ROM1 RP1 RP1L1 RP2 RP9 RPE65
RPGR RPGRIP1 RREB1 RTL1 RTTN SAG SCAPER SDHA SDHAF2
SDHB SDHC SDHD SEC24C SELENOI SEMA4A SERPINC1 SETD2
SLC24A1 SLC25A11 SLC37A4 SLC6A6 SLC7A14 SMAD4 SMCHD1
SMPD1 SNRNP200 SPATA7 SSBP1 STN1 STX1A TBL2 TBX1 TLCD3B
TMEM127 TMEM231 TMEM270 TOPORS TREX1 TSPAN12 TTC8 TUB TULP1 UFD1 UNC119 USH2A USP45
VHL VPS37D WDR19 WT1 YME1L1 ZNF408 ZNF513]

HP_PREMATURE_CORONARY_ARTERY_ATHEROSCLEROSIS > This term refers a gene set that is related to the premature development of atherosclerosis in the coronary arteries, which can lead to coronary artery disease (CAD). [ABCA1 ABCG5 ABCG8 ACTA2
APOA1 APOB APOE CEP19 CYP27A1 ERCC6 ERCC8 GPIHBP1 LDLR LDLRAP1 LIPC
LMNA LRP6 MEF2A PCSK9]

ST_WNT_BETA_CATENIN_PATHWAY > This identifier refers to a gene pathway involved in the Wnt/beta-catenin signaling. The Wnt/beta-catenin pathway is crucial for various cellular processes, including development, cell proliferation, and differentiation. [AKT1 AKT2 AKT3
ANKRD6 APC AXIN1 AXIN2 CBY1 CER1 CSNK1A1 CTNNB1 CXXC4 DACT1
DKK1 DKK2 DKK3 DKK4 DVL1 FRAT1 FSTL1 GSK3A GSK3B LRP1 MVP NKD1 NKD2 PIN1 PSEN1 PTPRA
RPSA SENP2 SFRP1 TSHB WIF1]

GOBP_WNT_SIGNALING_PATHWAY_INVOLVED_IN_MIDBRAIN_DOPAMINERGIC_NEURON_DIFFERENTIATION
> This identifier contains genes that are related to the role of the Wnt signaling pathway in the differentiation of dopaminergic neurons in the midbrain. This process is important for the development of the nervous system and is particularly relevant to the study of diseases like schizophrenia and Parkinson's disease, where dopaminergic neurons are affected. [CSNK1D CSNK1E CTNNB1 FZD1 LRP6 RYK WNT1 WNT2 WNT3 WNT3A WNT5A WNT9B]

GOBP_POSITIVE_REGULATION_OF_DOPAMINE_RECEPTOR_SIGNALING_PATHWAY > This identifier contains genes responsible for a biological process that positively regulates the signaling pathway of dopamine receptors. Dopamine receptors are critical for many neurological processes, and their signaling pathways are important in the context of neurological diseases, e.g. schizophrenia and Parkinson's disease. [CAV2 DRD3 LRRK2 PRMT5 VPS35]

Supplementary Tables

Table S1*Robust regression results for inner and outer retina*

Phenotype	Coef	CI(low)	CI(high)	SE	BPstat	BPp	F	p
RNFL mean	-0.017	-0.062	0.028	0.02297	66.05	p < .001	0.53	0.46635
GC IPL mean	-0.087	-0.149	-0.026	0.03134	28.37	p = 0.164	7.76	0.00534
INL mean	-0.004	-0.03	0.021	0.0131	49.26	p < .001	0.11	0.73716
INL RPE mean	-0.101	-0.184	-0.018	0.04242	53.87	p < .001	5.64	0.01755

Table S2*Association between polygenic risk for schizophrenia and macular subfields*

Macular subfield	hm	Coef	CI(low)	CI(high)	SE	BPstat	BPp	F	p	pFWE	Groups
Inner Inferior left	left	-0.0090831	-0.016	-0.002	0.00351	67.95	p < .001	6.69	0.00971	0.09710	Inner Inferior
Inner Inferior right	right	-0.0111756	-0.018	-0.004	0.00346	53.37	p < .001	10.39	0.00127	0.02032	Inner Inferior
Outer Inferior left	left	-0.0022769	-0.01	0.005	0.00382	59.74	p < .001	0.36	0.55125	1.00000	Outer Inferior
Outer Inferior right	right	-0.0035174	-0.011	0.004	0.00389	47.46	p = 0.001	0.82	0.36596	1.00000	Outer Inferior
Inner Nasal left	left	-0.0108702	-0.018	-0.004	0.00356	59.65	p < .001	9.30	0.00229	0.03435	Inner Nasal
Inner Nasal right	right	-0.0128938	-0.02	-0.006	0.00365	48.59	p < .001	12.43	0.00042	0.00756	Inner Nasal
Outer Nasal left	left	-0.0074260	-0.015	0	0.00394	47.12	p = 0.001	3.55	0.05948	0.41636	Outer Nasal
Outer Nasal right	right	-0.0114548	-0.019	-0.004	0.00393	43.29	p = 0.004	8.48	0.00360	0.04320	Outer Nasal
Inner Superior left	left	-0.0102455	-0.017	-0.004	0.0034	68.31	p < .001	9.07	0.00259	0.03435	Inner Superior
Inner Superior right	right	-0.0117573	-0.019	-0.005	0.00353	54.37	p < .001	11.07	0.00088	0.01496	Inner Superior
Outer Superior left	left	-0.0100111	-0.017	-0.003	0.00366	57.77	p < .001	7.48	0.00624	0.06864	Outer Superior
Outer Superior right	right	-0.0108973	-0.018	-0.004	0.00359	54.48	p < .001	9.20	0.00243	0.03435	Outer Superior
Inner Temporal left	left	-0.0084811	-0.015	-0.002	0.00339	71.5	p < .001	6.26	0.01234	0.11106	Inner Temporal
Inner Temporal right	right	-0.0082580	-0.015	-0.001	0.00346	51.55	p < .001	5.70	0.01696	0.13568	Inner Temporal
Outer Temporal left	left	-0.0067490	-0.014	0	0.00365	44.36	p = 0.003	3.42	0.06450	0.41636	Outer Temporal
Outer Temporal right	right	-0.0050174	-0.013	0.003	0.00384	46.66	p = 0.002	1.71	0.19096	0.95480	Outer Temporal
Central left	left	-0.0032214	-0.012	0.005	0.00433	65.13	p < .001	0.55	0.45765	1.00000	Central
Central right	right	-0.0040272	-0.013	0.005	0.00448	66.62	p < .001	0.81	0.36926	1.00000	Central

Table S3*Association between polygenic risk for schizophrenia (PRSSZ) at different p-value thresholds and mean macular thickness*

PRS	Phenotype	Coef	CI(low)	CI(high)	SE	F	p	pFWER
PRSSZ	Macula mean	-0.17	-0.31	-0.029	0.07159	5.59	0.0181	0.0181
PRSSZ 0.001	Macula mean	-0.10	-0.238	0.046	0.07259	1.75	0.1857	0.1857
PRSSZ 0.05	Macula mean	-0.18	-0.345	-0.024	0.08199	5.06	0.0244	0.0244
PRSSZ 0.1	Macula mean	-0.16	-0.325	0.007	0.08454	3.53	0.0601	0.0601
PRSSZ 0.2	Macula mean	-0.16	-0.329	0.003	0.08468	3.70	0.0544	0.0544
PRSSZ 0.3	Macula mean	-0.15	-0.322	0.012	0.08538	3.28	0.0699	0.0699
PRSSZ 0.4	Macula mean	-0.16	-0.322	0.011	0.08512	3.33	0.068	0.0680
PRSSZ 0.5	Macula mean	-0.15	-0.313	0.02	0.08501	2.98	0.0846	0.0846
PRSSZ 1	Macula mean	-0.15	-0.317	0.016	0.08488	3.13	0.0769	0.0769

Table S4

Permutation test regression between polygenic risk for schizophrenia enriched for multiple gene pathways and inner vs. outer retinal thickness at p-value threshold 1 using PRSet.

Pathway	GeseaPathwayCode	Num_SNP	Phenotype	Estimate	SE	selfcontained.p	competitive.p	Groups	Clhigh	Clow
ABNOVAS PRS	M43559	2267	GCIPL	-0.0216670	0.0370876	0.5590830	0.5983400	Microvasculature	0.051	-0.094
ABNOVAS PRS	M43559	2267	INL	0.0036801	0.0163518	0.8219350	0.8336170	Microvasculature	0.036	-0.028
ABNOVAS PRS	M43559	2267	INLRPE	-0.0175006	0.0629268	0.7809300	0.7873210	Microvasculature	0.106	-0.141
ABNOVAS PRS	M43559	2267	RNFL	0.0201864	0.0261130	0.4395030	0.4640540	Microvasculature	0.071	-0.031
ACUTEINFLAM PRS	M6557	816	GCIPL	-0.0507433	0.0371047	0.1714560	0.2003800	Inflammation	0.022	-0.123
ACUTEINFLAM PRS	M6557	816	INL	0.0153199	0.0163595	0.3490450	0.3770620	Inflammation	0.047	-0.017
ACUTEINFLAM PRS	M6557	816	INLRPE	-0.0901261	0.0629553	0.1522710	0.1643840	Inflammation	0.033	-0.214
ACUTEINFLAM PRS	M6557	816	RNFL	0.0366421	0.0261250	0.1607560	0.1784820	Inflammation	0.088	-0.015
CATENIN PRS	M17761	342	GCIPL	-0.0626347	0.0368550	0.0892364	0.1145890	Developmental	0.010	-0.135
CATENIN PRS	M17761	342	INL	-0.0180391	0.0162495	0.2669520	0.2876710	Developmental	0.014	-0.050
CATENIN PRS	M17761	342	INLRPE	-0.0008908	0.0625345	0.9886350	0.9900010	Developmental	0.122	-0.123
CATENIN PRS	M17761	342	RNFL	-0.0342921	0.0259497	0.1863500	0.2033800	Developmental	0.017	-0.085
CHROINFLAM PRS	M15140	137	GCIPL	0.0135218	0.0374524	0.7180730	0.7288270	Inflammation	0.087	-0.060
CHROINFLAM PRS	M15140	137	INL	0.0046204	0.0165125	0.7796230	0.7938210	Inflammation	0.037	-0.028
CHROINFLAM PRS	M15140	137	INLRPE	-0.0737256	0.0635442	0.2459660	0.2697730	Inflammation	0.051	-0.198
CHROINFLAM PRS	M15140	137	RNFL	0.0393136	0.0263690	0.1359980	0.1502850	Inflammation	0.091	-0.012
CORART PRS	M36658	244	GCIPL	0.0043803	0.0372143	0.9063020	0.9100090	Microvasculature	0.077	-0.069
CORART PRS	M36658	244	INL	0.0079957	0.0164075	0.6260350	0.6457350	Microvasculature	0.040	-0.024
CORART PRS	M36658	244	INLRPE	0.0401633	0.0631410	0.5247230	0.5439460	Microvasculature	0.164	-0.084
CORART PRS	M36658	244	RNFL	-0.0164771	0.0262021	0.5294540	0.5418460	Microvasculature	0.035	-0.068
DOPPOSREG PRS	M24111	69	GCIPL	0.0124878	0.0381142	0.7431860	0.7448260	Developmental	0.087	-0.062
DOPPOSREG PRS	M24111	69	INL	-0.0061939	0.0168043	0.7124350	0.7360260	Developmental	0.027	-0.039
DOPPOSREG PRS	M24111	69	INLRPE	-0.0103033	0.0646684	0.8734130	0.8795120	Developmental	0.116	-0.137
DOPPOSREG PRS	M24111	69	RNFL	0.0300539	0.0268354	0.2627500	0.2787720	Developmental	0.083	-0.023
NEUROINFLAM PRS	M24927	751	GCIPL	-0.0958475	0.0391102	0.0142630	0.0230977	Inflammation	-0.019	-0.173
NEUROINFLAM PRS	M24927	751	INL	-0.0061076	0.0172450	0.7232160	0.7412260	Inflammation	0.028	-0.040
NEUROINFLAM PRS	M24927	751	INLRPE	-0.0093058	0.0663644	0.8884850	0.8903110	Inflammation	0.121	-0.139
NEUROINFLAM PRS	M24927	751	RNFL	-0.0197093	0.0275395	0.4741970	0.4941510	Inflammation	0.034	-0.074
TGFB PRS	M18933	816	GCIPL	-0.0507433	0.0371047	0.1714560	0.2043800	Inflammation	0.022	-0.123
TGFB PRS	M18933	816	INL	0.0153199	0.0163595	0.3490450	0.3800620	Inflammation	0.047	-0.017
TGFB PRS	M18933	816	INLRPE	-0.0901261	0.0629553	0.1522710	0.1700830	Inflammation	0.033	-0.214
TGFB PRS	M18933	247	RNFL	0.0100906	0.0267023	0.7055140	0.7214280	Inflammation	0.062	-0.042
WNT PRS	M25305	107	GCIPL	-0.0303761	0.0386493	0.4319080	0.4606540	Developmental	0.045	-0.106
WNT PRS	M25305	107	INL	0.0232558	0.0170399	0.1723300	0.1992800	Developmental	0.057	-0.010
WNT PRS	M25305	107	INLRPE	-0.0128762	0.0655768	0.8443340	0.8482150	Developmental	0.116	-0.141
WNT PRS	M25305	107	RNFL	-0.0339460	0.0272122	0.2122400	0.2231780	Developmental	0.019	-0.087

Supplementary Figures

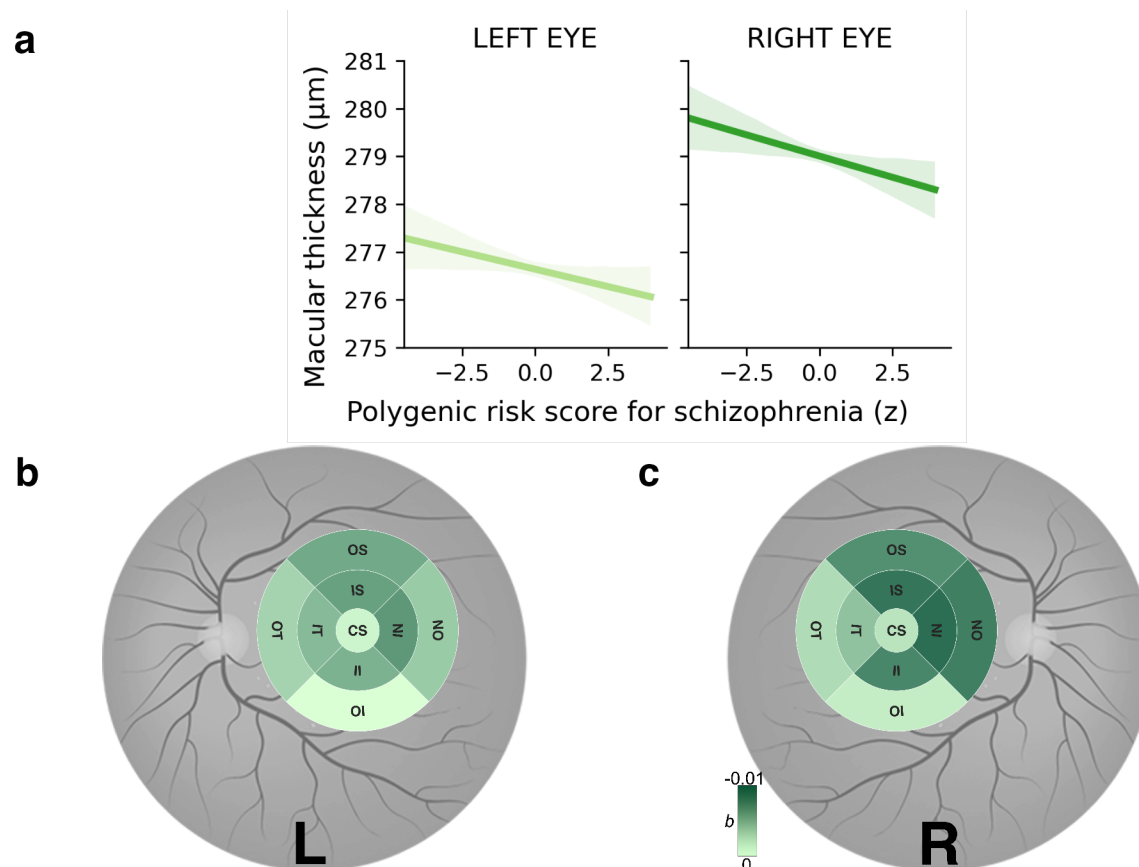


Figure S1. a. Association between polygenic risk score for schizophrenia and overall macular thickness in each eye respectively. Solid lines represent the regression estimates, while complementary shaded areas correspond to 95 percent confidence intervals. Individual macular subfields associated with polygenic risk scores for schizophrenia for both left eye (b) and right eye (c). Color coding corresponds to coefficients from robust linear regression model. Higher b values correspond to thinner macular subfields with increasing polygenic risk scores for schizophrenia. The sizes of subfields are slightly inflated for visualization purposes only. CS: Center subfield, IS: Inner Superior, OS: Outer Superior, IN: Inner Nasal, ON: Outer Nasal, II: Inner Inferior, OI: Outer Inferior, IT: Inner Temporal, OT: Outer Temporal.

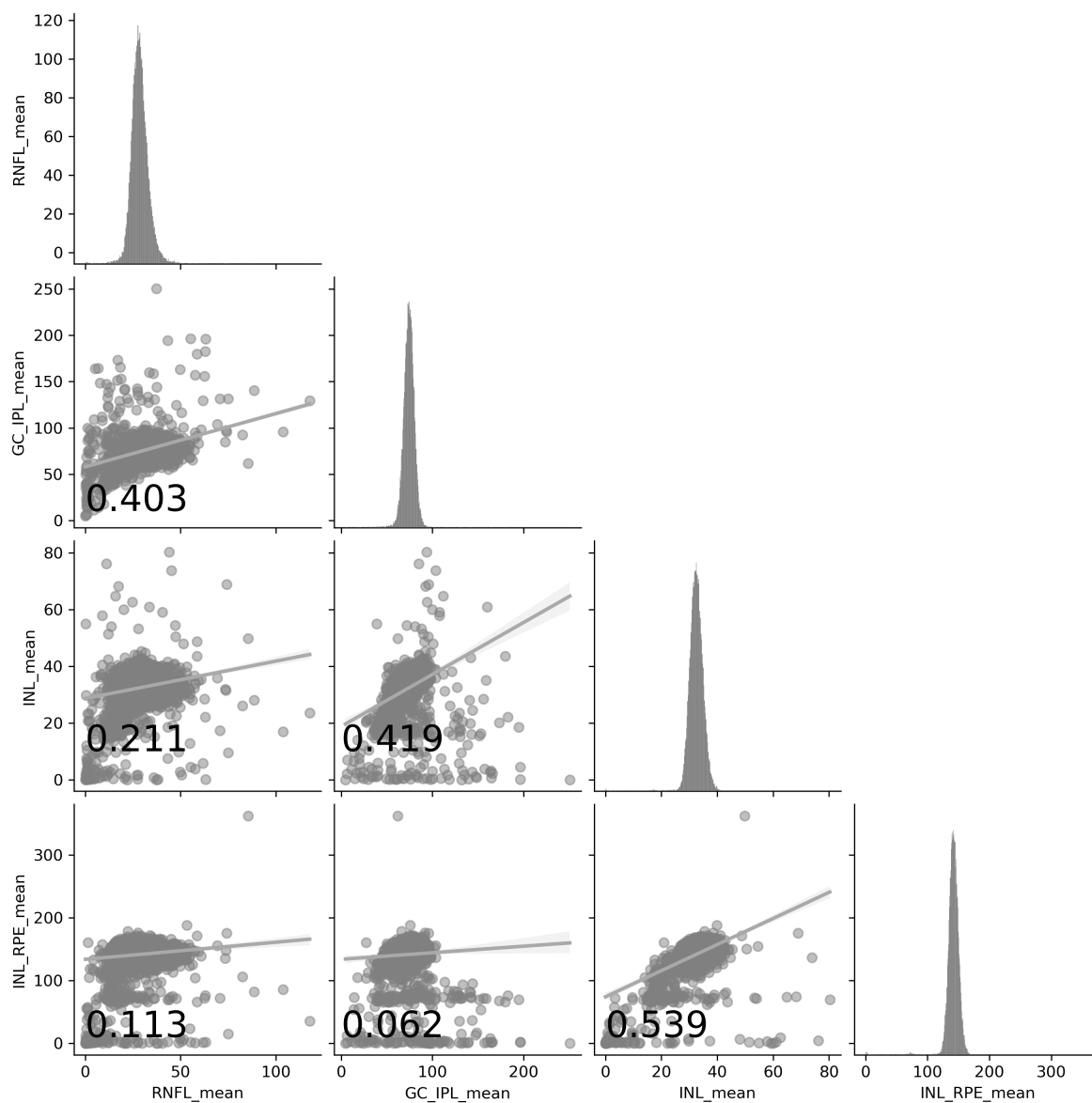


Figure S2. Pearson correlation coefficients between retinal phenotypes and showing their individual distribution.

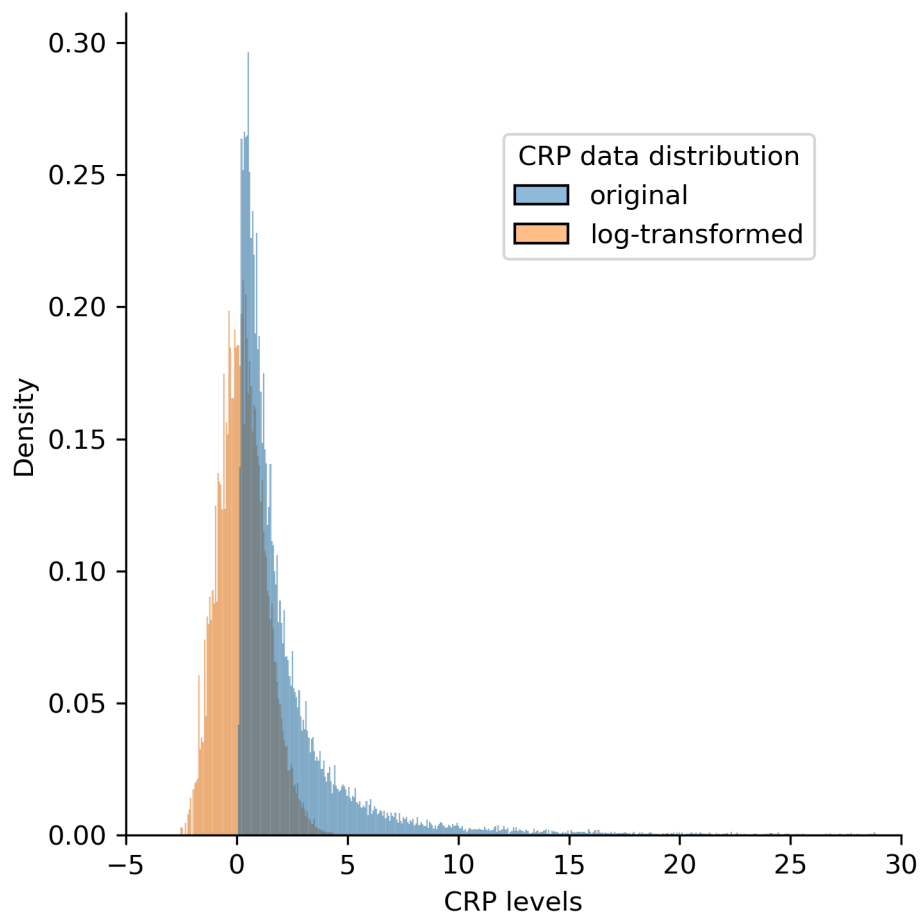


Figure S3. Logarithmic transformation of CRP measurements